Synthesis and Protein Adsorption Resistance of PEG-Modified Poly(*N*-isopropylacrylamide) Core/Shell Microgels

Daoji Gan and L. Andrew Lyon*

School of Chemistry and Biochemistry, Georgia Institute of Technology, Atlanta, Georgia 30332-0400

Received July 23, 2002; Revised Manuscript Received October 23, 2002

ABSTRACT: Thermoresponsive poly(*N*-isopropylacrylamide) (pNIPAm) nanoparticles grafted with poly(ethylene glycol) (PEG) chains were prepared via free-radical precipitation polymerization, using PEG monomethyl ether monomethacrylate (PEG-MA) as a comonomer. The breadth of the particle size distributions was found to increase with the amounts of the PEG-MA used, along with a broadening of the volume phase transition of the particles and a transition shift to higher temperatures. However, these effects were minimized by spatially localizing the PEG to the particle periphery in core−shell pNIPAm particles prepared using a two-stage precipitation polymerization method. Reduced protein adsorption on the particle surface was observed as a result of incorporation of PEG chains into the particles, especially when the PEG chains were located in the particle shell. The protein adsorption measurements also suggest that the PEG side chains may stretch outward from the particle surface as the particles collapse at temperature above the transition temperature. The increased mobility of the PEG chains, presumably due to this surface extension, was confirmed by variable temperature ^{1}H NMR studies for both core and core−shell particles. Such effects are also observed for particles where the PEG chains are localized in the particle core, which is then surrounded by a pNIPAm shell. These results suggest that the PEG grafts can penetrate the pNIPAm shell when it is in its phase-separated state.

Introduction

Stimuli-responsive polymers, including cross-linked monolithic and particulate gels of such macromolecules, have been employed in numerous potential applications, including drug delivery,[1−6] chromatographic separations,[7−9] cell culture systems,[10,11] and catalysis.[12,13] Among these, thermally sensitive polymers based on poly(*N*-alkylacrylamide)s, especially poly(*N*-isopropylacrylamide) (pNIPAm), have been most heavily studied.[14,15] PNIPAm exhibits a reversible phase separation in aqueous media at its lower critical solution temperature (LCST) around 31 °C.[15] As the temperature of the pNIPAm/water solution exceeds the LCST, the chains of pNIPAm undergo a "coil-to-globule" transition due to dissociation of water from the polymer chains and concomitant polymer self-association.[16] PNIPAm microgels, which are submicron-sized, cross-linked latex particles usually prepared by free-radical precipitation polymerization, differ from macrogels in a number of respects.[14] Microgels display colloidal behavior and have a high surface-to-volume ratio that is several orders of magnitude larger than that of a comparable macrogel. Varied physical properties of microgel suspensions can be modulated by the phase transition, including the particle hydrophobicity, size, scattering cross section, and electrophoretic mobility of the latex.[17−21] By obtaining a high degree of control over these properties and the stimuli that induce property changes, complex polymer structures designed for specific applications may be assembled. Along these lines, core−shell and core−corona particles have been constructed either to spatially localize chemical functionalities to a defined position, to render thermoresponsivity to nonresponsive particles, or to modify specific physical properties of the particles.[20,22−27]

Recently, our group has developed methods for the preparation of pNIPAm microgels with a core−shell morphology.[28−32] In these studies, we have shown that multiresponsive behavior and multiple phase transitions can be imparted to core−shell particles. Incorporation of hydrophobic comonomer units into the particles has also been shown to significantly change the particle deswelling kinetics. In this paper, we report synthesis of pNIPAm nanoparticles using a PEG macromonomer as a comonomer. Since PEG is more hydrophilic than pNIPAm,[33,34] especially at elevated temperature, incorporation of PEG chains into the microgel is expected to thus change hydrophobic/hydrophilic character of pNIPAm particles as a function of temperature. It is also expected that PEG chains will render the particles resistant to protein adsorption, in view of the characteristics of PEG chains in aqueous environment.[35,36] Finally, the effect of PEG localization in either the particle core or shell is investigated with respect to phase transition behavior and temperature-dependent protein adsorption.

Experimental Section

Materials. All chemicals were obtained from Aldrich unless otherwise noted. *N*-Isopropylacrylamide (NIPAm) was recrystallized from hexane (J. T. Baker) prior to use. *N*,*N*′-Methylenebis(acrylamide) (BIS), sodium dodecyl sulfate (SDS), ammonium persulfate (APS), poly(ethylene glycol) monomethyl ether monomethacrylate (PEG-MA) (PEG MW = 1000, Polysciences, Inc.), and Bradford Reagent were used as received. Bovine serum albumin (BSA) was purchased from Sigma. Water used in all experiments was distilled and then purified using a Barnstead E-Pure system operating at a resistance of 18 MΩ. A 0.2 μm filter was incorporated into this system to remove particulate matter.

Polymerization. The pNIPAm-based particles were prepared via free radical precipitation polymerizations, using APS (1 mol % based on the monomer, NIPAm) as an initiator and BIS (5 mol %) as a cross-linker. 1 mol % SDS was added as a surfactant, and the final concentration of NIPAm in water was 7.5 mg/mL. To prepare the particles having PEG side chains, various amounts of PEG-MA (0−40 wt % based on NIPAm) were introduced to the reaction batch. Prior to polymerization,

10.1021/ma021186k CCC: $22.00 © 2002 American Chemical Society
Published on Web 11/21/2002

Table 1. Chemical Compositions, Particle Sizes, and Size Distributions of PNIPAm Microgels Copolymerized with PEG Macromonomers

	core							
	PEG %[b]				shell PEG %[b]		core−shell	
sample[a]	wt %	mol %	*R*, nm[c]	polyd[c]	wt %	mol %	*R*, nm[c]	polyd[c]
C10	10	1.05	126 ± 4	23 ± 1				
C20	20	2.10	164 ± 8	30 ± 3				
C40	40	4.21	152 ± 6	42 ± 4				
C0	0	0	145 ± 8	18 ± 2				
C0-S5	0	0	145 ± 8	18 ± 2	5	0.53	169 ± 7	20 ± 3
C5	5	0.53	131 ± 2	22 ± 2				
C5-S0	5	0.53	131 ± 2	22 ± 2	0	0	164 ± 4	24 ± 1

[a] In the sample code, C and S stand for particle core and shell, respectively, while the number following each letter represents the weight percentage of PEG introduced into either core or shell. [b] Feed ratio based on NIPAm used for polymerization. [c] Average of five replicate measurements by PCS at 25 °C in water suspension, wherein R denotes hydrodynamic radii of particles and polyd is the percentage polydispersity.

the temperature of reaction mixture was raised to, and then kept at, 70 °C with continuous nitrogen bubbling for 2 h. The polymerization was initiated by addition of APS and then carried out at 70 °C under a nitrogen atmosphere for 6 h. The particles were purified via dialysis against water for 14 days, with daily replacement of the dialyzed liquid with fresh water.

The core−shell particles were prepared via a two-stage (seed and feed) polymerization. A detailed procedure for this polymerization has been described elsewhere.[28,29,31] In brief, the particle suspension prepared by the method described above (first stage) was used as seed particles. A second feed of monomer, PEG-MA (if necessary), cross-linker, and surfactant were then introduced to this particle suspension. After nitrogen was bubbled into the reaction mixture at 70 °C for 2 h, the second-stage polymerization was initiated via addition of APS and again carried out at 70 °C for 6 h. It should be emphasized that the first batch of hydrogel particles (core) served as nuclei, around which the polymer chains preferentially grow in the second stage of polymerization (shell addition).[28,31] The particles were also purified by the dialysis procedure mentioned above. The chemical compositions and particle size information are listed in Table 1.

Photon Correlation Spectroscopy (PCS). The particle sizes and size distributions in aqueous solutions were measured by PCS (Protein Solutions, Inc.).[31,37] A Peltier device integrated into the cuvette holder was used to control the solution temperature, yielding temperature accuracy within ±0.1 °C. Prior to taking measurements, the particle solutions were allowed to thermally equilibrate at each temperature for 10 min. Longer equilibration times did not lead to variations in the observed hydrodynamic radii, polydispersities, or scattering intensities. Hydrodynamic radii of the particles were calculated from diffusion coefficients using the Stokes−Einstein equation. All correlogram analyses were performed with manufacturer-supplied software (Dynamics v.5.25.44, Protein Solutions, Inc.). The data presented below are the averaged values of 20 measurements, with a 15 s integration time for each measurement. The volume deswelling ratios (V/V^*) of the particles were calculated via the relation $V/V^* = (R^3 - R^{*3})/R^{*3}$, where R and R^* are the PCS measured particle radii at the measured temperature and at 25 °C, respectively.

Protein Adsorption Experiments. The concentration of BSA in aqueous solution can be determined by the Bradford procedure,[38] which is based on the formation of a complex between a dye, Brilliant Blue G, and a protein in solution. The protein−dye complex causes a shift in the absorption maximum of the dye from 465 to 595 nm, with the absorption intensity at 595 nm being proportional to the concentration of protein in solution. To determine the amount of protein absorbed on the particles, a mixture of hydrogel particles (0.1 mg/mL) and BSA (1.0 mg/mL) in phosphate buffer solution (PBS, pH = 7.0) was prepared and incubated at a designated temperature that was controlled by a water bath. An aliquot of the mixture was removed and centrifuged at a scheduled time. The amount of protein remaining in the supernatant was determined by the Bradford method described above. The absorbed BSA on the particles was thus calculated by subtracting the amount of protein in the supernatant from that in the original solution and converted to a value of mg of protein/mg of particles.

^{1}H NMR. A Varian Unity 300 MHz NMR spectrometer was used to determine the chemical compositions of the hydrogel particles. The freeze-dried particles were redispersed in D_2O, and the spectra were then recorded at 25 and 42 °C. Before taking measurements, the solution was allowed thermally equilibrate for 10 min at each temperature. No changes in the signal intensities were observed if the equilibration time was prolonged.

Results and Discussion

In this work, PEG-MA has been used as a comonomer in order to covalently attach macromolecular side chains to the pNIPAm-based microgel particles. PEG is well-known to provide protein adsorption resistance;[35,36] thus, the incorporation of PEG chains into the microgels might be expected to minimize nonspecific interactions of the particles with biological environments. In aqueous solution, the PEG oxygens form hydrogen bonds with water, providing the PEG segments with a protective hydration shell that efficiently prevents hydrophobically driven protein adsorption.[35,36] In addition, the large excluded volume and chain mobility of PEG segments result in steric hindrance that is believed to be partially responsible for the resistance to protein adsorption.[39,40] Furthermore, PEG is more hydrophilic than pNIPAm even at room temperature;[33,34] thus, the incorporation of PEG should also change the hydrophobic/hydrophilic balance of the particles and thus phase transition behavior. This study is therefore designed to elucidate the effects of PEG side chain content and location on the phase transition and protein adsorption behavior of core and core−shell pNIPAm-based particles.

The particle size variations of a series of pNIPAm microgels containing various PEG concentrations were measured as a function of temperature in water by PCS (Figure 1); the monomer ratios used in the preparation of these particles are listed in Table 1. Although these particles contain up to 40 wt % grafted PEG chains, a temperature-induced particle size decrease is still observable in the range between 25 and 42 °C for all the particles (Figure 1a). To better visualize phase transition differences between particles of different radii, the size variations have been normalized to deswelling volume ratios as described in the Experimental Section. As such, modulation of the phase transition behavior as a function of PEG content is clearly illustrated in the volume-normalized curves shown in Figure 1b. The transition not only shifts to higher temperatures but also broadens as the PEG-MA concentration is increased. Furthermore, the magnitudes of the deswelling ratios are significantly decreased with increased PEG-MA content. These types of changes in phase transition behavior have also been observed when other hydrophilic monomers were copolymerized with the NIPAm monomer.[31,41] Hydrophilic comonomer units may decrease the propensity for hydrophobic association of isopropyl groups of pNIPAm segments, thus leading to broader phase transitions that occur at higher temperatures. Interestingly, although the original particle size distribution increases with PEG content, the polydispersities of the particles do not change with the solution temperature (Figure 1c). This suggests that the particles

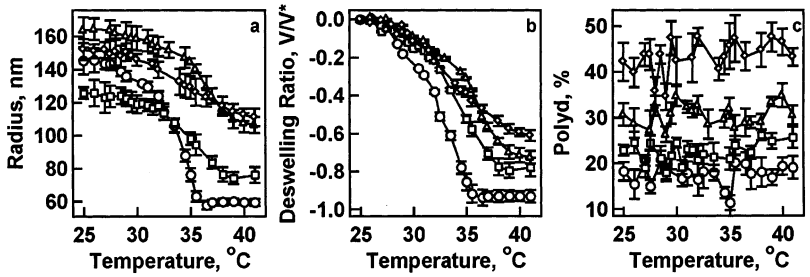

Figure 1. PCS measured temperature dependence (average value of five measurements) of hydrodynamic radii (panel a), deswelling ratios (panel b), and polydispersities (panel c) of pNIPAm microgels (sample C0-C40) with various contents of grafted PEG chains: C0, ○; C10, □; C20, ◇; C40, △. See Table 1 for synthetic details.

obtained at the completion of polymerization are stable and do not form aggregates at elevated temperatures.

While the phase transition behavior of the pNIPAm-*co*-PEG microgels are easily interpreted in terms of polymer hydrophobic/hydrophilic balance, it is disconcerting that the polydispersities of these particles tend toward 45% at 40 wt % PEG. Only for low PEG content microgels can the particles be considered monodispersed. This trend toward higher polydispersity can be explained if one considers the mechanism of microgel formation. As described above, microgel particles were prepared by free-radical precipitation polymerization using APS as an initiator. Prior to addition of initiator, the reaction mixture is a homogeneous and transparent solution since all components (monomer, comonomer, surfactant, and cross-linker) are fully soluble in water. Approximately 5 min after introduction of initiator to this reaction mixture at 70 °C the reaction solution turns faintly turbid. As the polymerization proceeds, the turbidity of the solution further increases to being milky. Given that the reaction temperature (70 °C) is much higher than the LCST (31 °C),[14] the growing polymer chains, once reaching a critical length, precipitate from the solution and form precursor particles.[42] This is the source of the increased turbidity early in the reaction. While the initiator renders these nuclei negatively charged, thus providing a degree of electrostatic stabilization, the precursor particles are generally not well stabilized due to a high surface-to-volume ratio and therefore aggregate with each other until the particle sizes are large enough to confer colloidal stability. By this mechanism of particle formation, one finds that the critical process in particle nucleation relates to the insolubility (and hence phase separation) of the growing polymer chains in the solvent, which is largely dependent on hydrophobicity of the polymer chains in this particular system. Introduction of the hydrophilic PEG macromonomer into the reaction system would be expected to diminish the hydrophobic character of the growing polymer chains at the reaction temperature. The growing oligomers thus must attain a higher degree of polymerization before precipitation occurs, thereby leading to slow particle nucleation and perhaps a low charge density at the particle surface. It is most likely these two factors lead to increased particle size distributions with increasing PEG-MA concentration (Table 1). In precipitation polymerization, slow nucleation increases polydispersity by producing a situation where the total particle number changes at a competing rate to particle growth. For ideally monodisperse particle preparations, it is desirable to have all particle nucleation events take place very early in the polymerization, with further propagation contributing only to particle growth and not to new nucleation events. Furthermore, the presumably low charge density on the particles may contribute to greater degrees of particle aggregation late in the polymerization and hence a greater polydispersity. Indeed, flocculation appears in the reaction solution when higher concentrations of the macromonomer are used, suggesting that aggregation is a factor contributing to polydispersity in these syntheses.

To minimize these effects and thus increase the monodispersity of the preparations, core−shell particles were prepared. Core−shell particles were also prepared to investigate the influence of PEG location (core vs shell) on the particle behavior. In these cases, pNIPAm-based microgels are used as seeds for the polymerization of pNIPAm-based shells, thereby providing preformed "seeds" for particle nucleation. Furthermore, where protein adsorption resistance is required, the PEG chains can presumably perform this function more efficiently if they are localized at the surface, thus making PEG-containing shells attractive for applications in biotechnology. Core−shell particles with PEG chains in either the core or shell were prepared by two-stage polymerization. The particles prepared at the first stage were used as seeds, to which a feed of monomer, cross-linker, and initiator was introduced. During the second stage of polymerization, the seed particles serve as nuclei, which then grow by diffusive capture of oligomers and by coagulation of small precursor particles produced in the continuous phase.[28,31,43] Theoretical predictions suggest that the total particle number remains constant (no new nucleation events) so that the core−shell morphology is formed and maintained, with the shell thickness being only a function of the amount of polymer produced during the second stage.[43] As evidence for core−shell morphology formation, the core−shell particles have significantly increased radii whereas almost no change in the particle size distribution is observed upon addition of particle shell (Table 1). If new particles were nucleated to a significant extent, the width of the particle size distribution should be strongly perturbed. When the introduced PEG macromonomers are kept at or below 5 wt % (based on NIPAm used), the particle size distributions are found to be lower than 25%, which is quite close to the value of the initial seed particles.

Shown in Figure 2 is the temperature dependence of the particle size and volume ratio for samples C5 and C5-S0. The phase transition shows a breadth (∼5 °C) and position that are quite similar to those of pure pNIPAm particles. Compared to the particle core (C5), the core−shell particles (C5-S0) show only a slight modulation of the phase transition when the particle size variations are normalized to the deswelling volume ratios (Figure 2b). The magnitude of the volume decrease of the PEG-containing particle core is slightly

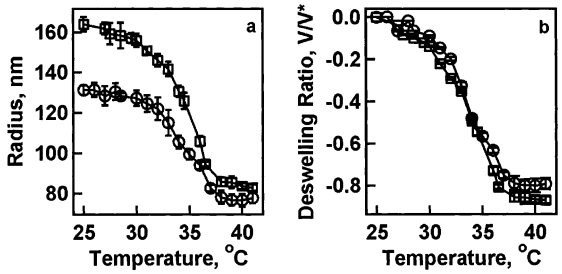

Figure 2. PCS measured particle radii (panel a) and thus calculated deswelling ratios (panel b) for sample C5 (○) and C5-S0 (□) as a function of solution temperature (average of five measurements).

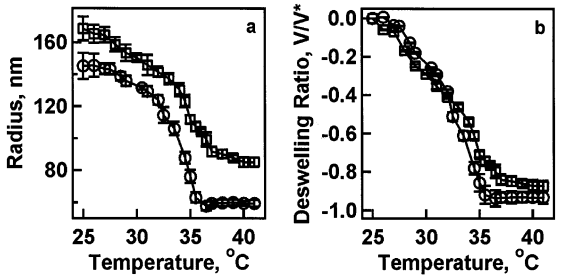

Figure 3. PCS measured particle radii (panel a) and calculated deswelling ratios (panel b) of sample C0 (○) and C0-S5 (□) as a function of solution temperature (average of five measurements).

smaller than that of the core−shell particles having a pure pNIPAm shell. This is in agreement with the argument that the inclusion of PEG in the particles should serve to decrease the efficacy of pNIPAm hydrophobic aggregation. The addition of a pure pNIPAm shell should increase the overall degree of deswelling in the particle. For comparison, another set of core−shell particles were constructed such that only the particle shell contains 5 wt % PEG chains, with the core seed being a simple BIS cross-linked pNIPAm microgel (samples C0 and C0-S5 in Table 1). Again, the formation of core−shell morphology is shown by the similar core and core−shell polydispersities (Table 1), as well as the increase in particle size for the core−shell particle (Figure 3a). Upon addition of the shell, the particles only show a slight shift of the transition to a higher temperature and a small decrease in the particle deswelling volume ratios (Figure 3b), due to the presence of PEG in the shell.

To measure nonspecific protein adsorption onto pNIPAm particles, bovine serum albumin (BSA) was used as a test protein and a standard Bradford assay was used to quantify the degree of adsorption. Figure 4 shows the BSA absorption onto pNIPAm particles (sample C0) as a function of assay time and as a function of temperature. When the protein adsorption is measured at a temperature (25 °C) that is below the volume phase transition temperature, BSA adsorption reaches a plateau of $\sim 5 \times 10^{-3}$ g of BSA/g of polymer after ~80 min. In contrast, at 42 °C the protein adsorption process is not observed to plateau even after 150 min, where the degree of adsorption has reached 11.6×10^{-3} g of BSA/g of polymer. It is interesting to note that this >2-fold increase in BSA adsorption occurs despite the fact that the particle surface area *decreases* by almost 7-fold from 25 to 42 °C. It is apparent from these results, as others have noted previously,[44] that deswollen pNIPAm is remarkably efficient at promoting the hydrophobic adsorption of proteins.

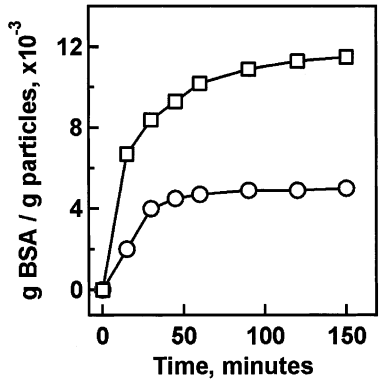

Figure 4. BSA adsorption on sample C0 as a function of incubation time at 25 (○) and 42 °C (□).

Table 2. Saturated BSA Adsorption and ^{1}H NMR Determined Peak Integrations, at 25 and at 42 °C, for PNIPAm Microgels Copolymerized with PEG Macromonomers

			integration ratios from ^{1}H NMR[b]			
	adsorbed BSA[a]		peak e/ peak a		peak e/ peak b	
sample	25 °C	42 °C	25 °C	42 °C	25 °C	42 °C
C10	3.7 ± 0.5	4.9 ± 0.4	0.17	0.25	1.1	1.4
C20	2.6 ± 0.4	2.9 ± 0.3	0.40	0.56	2.1	2.7
C40	1.2 ± 0.5	1.3 ± 0.2	0.67	0.77	3.9	4.3
C0	5.1 ± 0.6	11.6 ± 0.7				
C0-S5	4.2 ± 0.3	3.8 ± 0.2	0.05	0.12	0.27	0.70
C5	3.7 ± 0.4	4.9 ± 0.4	0.10	0.11	0.54	0.70
C5-S0	4.9 ± 0.7	6.7 ± 0.5	0.04	0.08	0.20	0.59

[a] 10^{-3} g of BSA absorbed on 1 g of particles; average value of five repeated measurements. [b] Peak e is the PEG methylene resonance; peaks a and b are the methyl and methylene protons, respectively, of isopropyl groups in pNIPAm segments (see Figure 6).

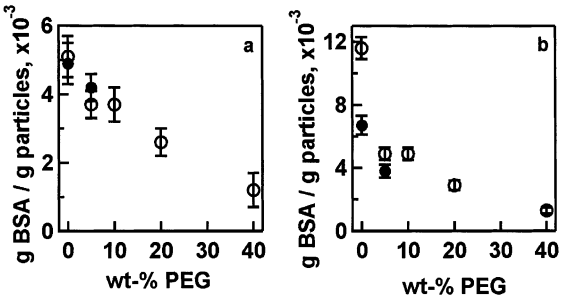

Figure 5. BSA adsorption (average of five replicated measurements) on pNIPAm-based particles as a function of temperature (panel a, 25 °C; panel b, 42 °C) and of PEG content introduced in the last stage of polymerization. The filled circles represent core−shell particles, while the open circles represent core particles (for details see Table 2).

The degrees of BSA adsorption at 150 min (at or near saturation) for all particles are listed Table 2 and displayed graphically in Figure 5. In Figure 5, the degree of BSA adsorption is plotted as a function of wt % PEG *in the last stage of the synthesis*. The filled circles in panels a and b represent the values for the two core−shell particles, where the PEG concentration is considered to be that present in the shell. For example, the C5-S0 sample is plotted as having 0 wt % PEG in Figure 5. This formalism allows the core−shell particles to be compared to the core particles on the basis of PEG localization in the particles. Indeed, Figure 5a (data taken at 25 °C) seems to show that this is an appropri-

ate approach, as the individual samples in each core−shell pair (C0/C5-S0 and C5/C0-S5) are statistically identical to each other with respect to BSA adsorption. Thus, it seems that simply localizing PEG at the particle surface is sufficient to inhibit protein adsorption. Furthermore, these data indicate that the incorporation of PEG chains into the particles significantly reduces the degree of BSA adsorption at 42 °C. For example, a more than 2-fold decrease in BSA adsorption at 42 °C is observed for particles containing only 10 wt % PEG chains (sample C10). It is further noteworthy that, in the case of core−shell particles, the *location* of PEG chains in the particles has a great influence on the degree of protein adsorption at 42 °C. A comparison of the data for samples C0-S5 and C5-S0 (Table 2 and Figure 5) shows that the low-temperature (25 °C) adsorption degree is nearly identical, while sample C0-S5 displays a 1.8-fold smaller propensity for protein adsorption than sample C5-S0 at 42 °C. Note that the total PEG concentrations are essentially the same for these two particles; the location of the PEG is the only significant variation between the two samples. A more compelling comparison is that between the 42 °C adsorption values for samples C0 and C5-S0. Despite both particles having surfaces that are composed largely of pNIPAm, the core−shell particle displays a 1.7-fold smaller degree of BSA adsorption than the pNIPAm core particle at 42 °C. It is apparent from these data that the inclusion of PEG in the core has the ability to modulate the surface hydrophobicity of the deswollen particle. The origin of this effect may stem from the synthesis conditions and the phase separation behavior of PEG and pNIPAm. First, since the PEG chains are much more hydrophilic than pNIPAm at the polymerization temperature (70 °C), it is reasonable to assume that the PEG chains tend to migrate to the particle surface during polymerization. Furthermore, these chains may be fully extended during shell synthesis, thereby resulting in a highly interpenetrated core−shell interface. However, the PEG chains located on the periphery of the particle core of sample C5-S0 should be too short to penetrate the surface of the shell to any significant degree at 25 °C, given that the shell thickness at that temperature is about 33 nm (Figure 2a). Therefore, the PEG core does not impact the low-temperature behavior of the particle. The shell thickness, however, decreases to about 6 nm at 42 °C (Figure 2a), which provides an opportunity for the PEG chains to penetrate the shell and approach the particle surface. In other words, as the particles collapse to a hydrophobic globule, the hydrophilic PEG chains may tend to phase separate from the pNIPAm and extend through the shell to maximize water−PEG interactions. This would lead to a relatively hydrophilic particle surface and therefore a reduction of protein adsorption at 42 °C.

To further investigate the possibility that topological changes in the microgels are responsible for the observed behavior, the proton NMR spectra of the particles in D_2O were monitored below and above the phase transition temperature. Shown in Figure 6 are representative ^1H NMR spectra of sample C20 at 25 and 42 °C. The proton assignments are consistent with the chemical structure of the polymer.[45,46] The peak at 1.10 ppm can be attributed to the methyl proton of the *N*-isopropyl group (peak a in Figure 6). A typical resonance for the methylene of the isopropyl group is observed at 3.8−4.0 ppm (peak b in Figure 6). The broad

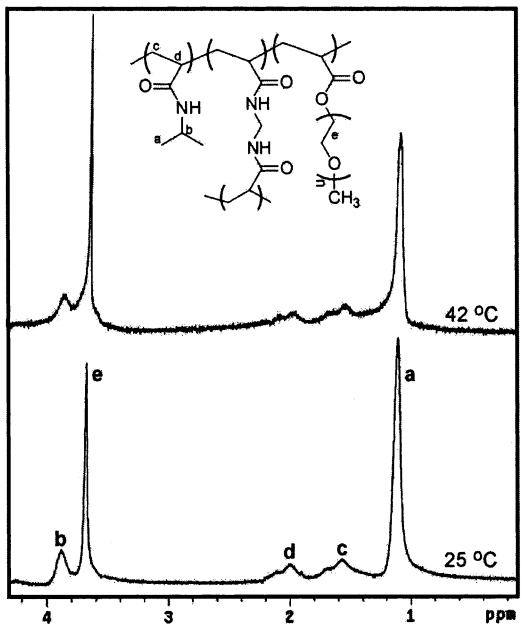

Figure 6. ^1H NMR spectra of sample C20 in D_2O measured at 25 and 42 °C.

peaks c and d are mainly due to protons on the polymer backbone. The characteristic methylene signal of the PEG side chains is located at 3.68 ppm (peak e in Figure 6), indicating a successful incorporation of the PEG chains into the particles. We did not detect the proton signal from the amide, which, as suggested by other authors,[46] may be due to a fast exchange with D_2O. In Figure 6, a comparison of the spectrum taken at 25 °C with that taken at 42 °C indicates that the relative intensity of peak e (PEG) increases, whereas peaks a and b decrease as the solution temperature is raised above the pNIPAm LCST. This suggests that when the particles deswell, the pNIPAm segments collapse to a dense, solidlike globule, thus decreasing their mobility. As a result, the relaxation time of some pNIPAm segments inside the particles becomes too short to be detected by the NMR technique,[46] leading to a broadening of the signals from the pNIPAm segments. In contrast, as the particles collapse to smaller hydrophobic entities, hydrophilic PEG side chains apparently separate from the globule, perhaps stretching outward from the surface, thus maintaining or increasing their relative mobility. Table 2 lists the integration ratios e/a and e/b for all particles used in this study. Note that all particles display an increase in these ratios as the temperature is raised to 42 °C, indicating that the PEG mobility is not strongly coupled to the pNIPAm mobility in the collapsed particles. This is true even for sample C5-S0, where the PEG is buried in the core beneath a layer of pNIPAm. Apparently, when the particle deswells, a significant fraction of the PEG chains are able to penetrate through the shell and extend outward from the particle surface to maintain a liquidlike mobility despite being covalently bound to the solidlike pNIPAm. These results correlate well with the BSA adsorption results for this particle, where the "buried" PEG was still able to significantly reduce the degree of adsorption at 42 °C.

Conclusions

Through copolymerization of NIPAm with the macromonomer PEG-MA, PEG side chains can be efficiently

incorporated into the responsive pNIAPm nanoparticles. Because of the more hydrophilic character of oligomers during polymerization, the particle size distributions increase as the amount of PEG-MA is increased. The incorporated PEG side chains also lead to a broader phase transition of the particles at a higher temperature, largely caused by the increased hydrophilicity of the particles and hence a lower propensity for pNIPAm to phase separate. Locating small amounts of PEG chains in a defined position on the particle (e.g., core−shell morphologies) can minimize these detrimental effects on the transition behavior. However, regardless of the preparation method, PEG side chains are able to reduce the propensity of bovine serum albumin to adsorb to the pNIPAm particles. This effect is most pronounced when the pNIPAm is phase-separated above its characteristic LCST. Indeed, even when the PEG is "buried" in a particle core surrounded by a pNIPAm shell, protein adsorption is inhibited above the LCST, suggesting that PEG modulates the particle surface hydrophobicity even when it is not purposely localized in the shell. NMR measurements reveal that for all particles the proton resonances associated with the PEG remain liquidlike when the pNIPAm signals broaden upon phase separation. Together, these results indicate that the PEG chains are able to phase separate and extend from the particle surface following pNIPAm deswelling, thus increasing the surface hydrophilicity even when in a buried architecture.

Acknowledgment. L.A.L. gratefully acknowledges financial support from the National Science Foundation, Division of Materials Research, and from the Arnold and Mabel Beckman Foundation for a Young Investigator Award.

References and Notes

(1) Kono, K.; Nakai, R.; Morimoto, K.; Takagishi, T. *Biochim. Biophys. Acta* **1999**, *1416*, 239−250.
(2) Moselhy, J.; Wu, X. Y.; Nicholov, R.; Kodaria, K. *J. Biomater. Sci., Polym. Ed.* **2000**, *11*, 123−147.
(3) Tuncel, A.; Ozdemir, A. *J. Biomater. Sci., Polym. Ed.* **2000**, *11*, 817−831.
(4) Kim, K. S.; Kim, J. M.; Kim, T. K. *Kongop Hwahak* **2000**, *11*, 133−137.
(5) Lin, H.-H.; Cheng, Y.-L. *Macromolecules* **2001**, *34*, 3710−3715.
(6) Kisera, P. F.; Wilson, G.; Needham, D. *J. Controlled Release* **2000**, *68*, 9−22.
(7) Kanazawa, H.; Yamamoto, K.; Matsushima, Y.; Takai, N.; Kikuchi, A.; Sakurai, Y.; Okano, T. *Anal. Chem.* **1996**, *68*, 100−105.
(8) Kanazawa, H.; Kashiwase, Y.; Yamamoto, K.; Matsushima, Y.; Kikuchi, A.; Sakurai, Y.; Okano, T. *Anal. Chem.* **1997**, *69*, 823−830.
(9) Yamamoto, K.; Kanazawa, H.; Matsushima, Y.; Takai, N.; Kikuchi, A.; Okano, T. *Chromatography* **2000**, *21*, 209−215.
(10) Kwon, O. H.; Kikuchi, A.; Yamato, M.; Sakurai, Y.; Okano, T. *J. Biomed. Mater. Res.* **2000**, *50*, 82−89.
(11) Yamato, M.; Kwon, O. H.; Hirose, M.; Kikuchi, A.; Okano, T. *J. Biomed. Mater. Res.* **2000**, *55*, 137−140.
(12) Bergbreiter, D. E.; Case, B. L.; Liu, Y.-S.; Caraway, J. W. *Macromolecules* **1998**, *31*, 6053−6062.
(13) Wang, G.; Kuroda, K.; Enoki, T.; Grosberg, A.; Masamune, S.; Oya, T.; Takeoka, Y.; Tanaka, T. *Proc. Natl. Acad. Sci. U.S.A.* **2000**, *97*, 9861−9864.
(14) Pelton, R. *Adv. Colloid Interface Sci.* **2000**, *85*, 1−33.
(15) Shibayama, M.; Tanaka, T. In *Advances in Polymer Science*; Springer-Verlag: Berlin, 1993; Vol. 109, pp 1−62.
(16) Wu, C.; Wang, X. *Phys. Rev. Lett.* **1998**, *80*, 4092−4094.
(17) Fernandez-Nieves, A.; Fernandez-Barbero, A.; Vincent, B.; de las Nieves, F. J. *Macromolecules* **2000**, *33*, 2114−2118.
(18) Fernandez-Nieves, A.; Fernandez-Barbero, A.; de las Nieves, F. J.; Vincent, B. *J. Phys.: Condens. Matter* **2000**, *12*, 3605−3614.
(19) Rasmusson, M.; Vincent, B.; Marston, N. *Colloid Polym. Sci.* **2000**, *278*, 253−258.
(20) Daly, E.; Saunders, B. R. *Phys. Chem. Chem. Phys.* **2000**, *2*, 3187−3193.
(21) Ohshima, H.; Makino, K.; Kato, T.; Fujimoto, K.; Kondo, T.; Kawaguchi, H. *J. Colloid Interface Sci.* **1993**, *159*, 512−514.
(22) Nabzar, L.; Duracher, D.; Elaissari, A.; Chauveteau, G.; Pichot, C. *Langmuir* **1998**, *14*, 5062−5069.
(23) Zhou, G.; Elaissari, A.; Delair, T.; Pichot, C. *Colloid Polym. Sci.* **1998**, *276*, 1131−1139.
(24) Matsuoka, H.; Fujimoto, K.; Kawaguchi, H. *Polym. J.* **1999**, *31*, 1139−1144.
(25) Senff, H.; Richtering, W.; Norhausen, C.; Weiss, A.; Ballauff, M. *Langmuir* **1999**, *15*, 102−106.
(26) Gilanyi, T.; Varga, I.; Meszaros, R.; Filipcsei, G.; Zrinyi, M. *Phys. Chem. Chem. Phys.* **2000**, *2*, 1973−1977.
(27) Dingenouts, N.; Seelenmeyer, S.; Deike, I.; Rosenfeld, S.; Ballauff, M.; Lindner, P.; Narayanan, T. *Phys. Chem. Chem. Phys.* **2001**, *3*, 1169−1174.
(28) Gan, D.; Lyon, L. A. *J. Am. Chem. Soc.* **2001**, *123*, 7511−7517.
(29) Gan, D.; Lyon, L. A. *J. Am. Chem. Soc.* **2001**, *123*, 8203−8209.
(30) Gan, D.; Lyon, L. A. *Polym. Prepr. (Am. Chem. Soc., Div. Polym. Chem.)* **2002**, *43*, 352−353.
(31) Jones, C. D.; Lyon, L. A. *Macromolecules* **2000**, *33*, 8301−8306.
(32) Wang, J.; Gan, D.; Lyon, L. A.; El-Sayed, M. A. *J. Am. Chem. Soc.* **2001**, *123*, 11284−11289.
(33) Virtanen, J.; Baron, C.; Tenhu, H. *Macromolecules* **2000**, *33*, 336−341.
(34) Virtanen, J.; Tenhu, H. *Macromolecules* **2000**, *33*, 5970−5975.
(35) Graham, N. B.; Zulfiqar, M.; Nwachuku, N. E.; Rashid, A. *Polymer* **1989**, *30*, 528−533.
(36) Graham, N. B.; Zulfiqar, M.; Nwachuku, N. E.; Rashid, A. *Polymer* **1990**, *31*, 909−916.
(37) Debord, J. D.; Lyon, L. A. *J. Phys. Chem. B* **2000**, *104*, 6327−6331.
(38) Bradford, M. M. *Anal. Biochem.* **1976**, *72*, 248−254.
(39) Amiji, M.; Park, K. *J. Biomater. Sci., Polym. Ed.* **1993**, *4*, 217−234.
(40) Ikada, Y. *Adv. Polym. Sci., Polym. Med.* **1984**, *57*, 103−140.
(41) Lowe, T. L.; Virtanen, J.; Tenhu, H. *Langmuir* **1999**, *15*, 4259−4265.
(42) Wu, X.; Pelton, R. H.; Hamielec, A. E.; Woods, D. R.; McPhee, W. *Colloid Polym. Sci.* **1994**, *272*, 467−477.
(43) Kawaguchi, S.; Winnik, M. A.; Ito, K. *Macromolecules* **1995**, *28*, 1159−1166.
(44) Kawaguchi, H.; Fujimoto, K.; Mizuhara, Y. *Colloid Polym. Sci.* **1992**, *270*, 53−57.
(45) Tokuhiro, T.; Amiya, T.; Mamada, A.; Tanaka, T. *Macromolecules* **1991**, *24*, 2936−2943.
(46) Larsson, A.; Kuckling, D.; Schonhoff, M. *Colloids Surf., A* **2001**, *190*, 185−192.

MA021186K